PCCP

PAPER

View Article Online
View Journal | View Issue

Cite this: *Phys. Chem. Chem. Phys.*, 2017, **19**, 28876

Exploring the effect of fluorinated anions on the CO_2/N_2 separation of supported ionic liquid membranes†

Andreia S. L. Gouveia, [ab] Liliana C. Tomé, [ab] Elena I. Lozinskaya, [c] Alexander S. Shaplov, [cd] Yakov S. Vygodskii[c] and Isabel M. Marrucho *[ab]

The CO_2 and N_2 permeation properties of ionic liquids (ILs) based on the 1-ethyl-3-methylimidazolium cation ($[C_2mim]^+$) and different fluorinated anions, namely 2,2,2-trifluoromethylsulfonyl-*N*-cyanoamide ($[TFSAM]^-$), bis(fluorosulfonyl) imide ($[FSI]^-$), nonafluorobutanesulfonate ($[C_4F_9SO_3]^-$), tris(pentafluoroethyl)trifluorophosphate ($[FAP]^-$), and bis(pentafluoroethylsulfonyl)imide ($[BETI]^-$) anions, were measured using supported ionic liquid membranes (SILMs). The results show that pure ILs containing $[TFSAM]^-$ and $[FSI]^-$ anions present the highest CO_2 permeabilities, 753 and 843 Barrer, as well as the greatest CO_2/N_2 permselectivities of 43.9 and 46.1, respectively, with CO_2/N_2 separation performances on top of or above the Robeson 2008 upper bound. The re-design of the $[TFSAM]^-$ anion by structural unfolding was investigated through the use of IL mixtures. The gas transport and CO_2/N_2 separation properties through a pure $[C_2mim][TFSAM]$ SILM are compared to those of two different binary IL mixtures containing fluorinated and cyano-functionalized groups in the anions. Although the use of IL mixtures is a promising strategy to tailor gas permeation through SILMs, the pure $[C_2mim][TFSAM]$ SILM displays higher CO_2 permeability, diffusivity and solubility than the selected IL mixtures. Nevertheless, both the prepared mixtures present CO_2 separation performances that are on top of or above the Robeson plot.

Received 14th September 2017,
Accepted 9th October 2017

DOI: 10.1039/c7cp06297d

rsc.li/pccp

Introduction

The development of supported ionic liquid membranes (SILMs) for CO_2 separation has been widely investigated in recent years mainly due to their easy preparation and versatility.[1–3] In contrast to traditional liquid membranes, which are produced by impregnating a porous membrane support with common organic solvents,[4] SILMs use ionic liquids (ILs) and thus benefit from negligible displacement of the liquid phase from the membrane pores through evaporation,[5,6] due to the low volatility of ILs.[7] It should also be emphasized that within the CO_2 separation context, the most important features of ILs are their high CO_2 affinity over light gases[8–10] and their inherent designer nature that enables the tailoring of IL properties by proper selection of cations and/or anions or *via* the addition of specific functional groups.

Numerous works have investigated the effect of IL chemical structure on the gas permeation properties of SILMs. A broad diversity of cations, such as imidazolium,[11] triazolium,[12] thiazolium,[13] pyridinium,[14] cholinium,[15] ammonium,[16] and phosphonium,[17] combined with halogens, sulfonates, carboxylates, fluorinated or cyano-functionalized anions, have been studied. Other works, mostly focusing on imidazolium-based ILs, have also explored the effect of alkyl,[18] fluoroalkyl,[19] etoxyalkyl,[20] and aminoalkyl[21]-functionalized cations. Since IL anions have a stronger influence on the CO_2 separation performance of SILMs than IL cations,[1] they deserved from the start a closer look. The first studies on SILMs made use of fluorinated anions such as bis(trifluoromethylsulfonyl)imide $[NTf_2]^-$, tetrafluoroborate $[BF_4]^-$, and hexafluorophosphate $[PF_6]^-$ and enabled drawing conclusions about the CO_2-phylic behaviour and high CO_2 permeabilities of these anions.[22] More recently, low viscous ILs with cyano-functionalized anions, such as tricyanomethanide $[C(CN)_3]^-$ and tetracyanoborate $[B(CN)_4]^-$,[23–25] have been recognized as better candidates for the development of improved SILMs, because of their superior CO_2 permeabilities and permselectivities when compared to the most used $[NTf_2]^-$ anion. Task-specific ILs bearing amine groups, such as those containing amino acid

[a] *Centro de Química Estrutural, Departamento de Engenharia Química, Instituto Superior Técnico, Universidade de Lisboa, Avenida Rovisco Pais, 1049-001 Lisboa, Portugal. E-mail: isabel.marrucho@tecnico.ulisboa.pt*
[b] *Instituto de Tecnologia Química e Biológica António Xavier, Universidade Nova de Lisboa, Av. da República, 2780-157 Oeiras, Portugal*
[c] *A. N. Nesmeyanov Institute of Organoelement Compounds Russian academy of sciences (INEOS RAS), Vavilov St., 28, 119991 Moscow, Russia*
[d] *Luxembourg Institute of Science and Technology (LIST), 5 avenue des Hauts-Fourneaux, L-4362, Esch-sur-Alzette, Luxembourg*

† Electronic supplementary information (ESI) available. See DOI: 10.1039/c7cp06297d

anions,[26–28] have also been proposed to prepare SILMs, since amine groups can chemically bond CO_2 and act as carriers for CO_2 facilitated transport through SILMs at low pressures. However, the high viscosity of these task-specific ILs is undoubtedly a key limitation, as CO_2 diffusion is strongly compromised.

In an effort to improve the CO_2 permeability and permselectivity properties of SILMs, our recent studies explored the use of IL mixtures by fixing the $[C_2mim]^+$ cation and researching on different anion chemical structures. Initially, SILMs based on IL mixtures combining anions with different CO_2 solubility behaviours were investigated: thiocyanate ($[SCN]^-$), dicyanamide ($[N(CN)_2]^-$) and bis(trifluoromethylsulfonyl)imide ($[NTf_2]^-$) that present physical solubility; acetate ($[Ac]^-$) and lactate ($[Lac]^-$), which additionally have chemical solubility.[29] Afterwards, we focused on IL mixtures based on sulfate ($[CH_3SO_4]^-$) and cyano-functionalized anions ($[SCN]^-$, $[N(CN)_2]^-$, $[C(CN)_3]^-$ and $[B(CN)_4]^-$).[30] Moreover, we studied IL mixtures containing $[C(CN)_3]^-$ and different amino acid anions, so that one IL component maintains the low viscosity, while the other provides the desired chemical characteristics for the active transport of CO_2.[31] The overall results of these studies showed that mixing anions with specific chemical features allows variations in IL viscosity and molar volume that significantly impact the gas transport through SILMs, and thus tailored permeabilities and permselectivities can be achieved.[29–31]

In the present work, the gas permeation properties and CO_2/N_2 separation performance of SILMs prepared with pure ILs bearing the $[C_2mim]^+$ cation and different less conventional fluorinated anions, namely $[TFSAM]^-$, $[FSI]^-$, $[C_4F_9SO_3]^-$, $[FAP]^-$ and $[BETI]^-$, were evaluated and the effect of the fluorinated moieties in the IL anion was discussed. Despite the fact that several SILMs with common fluorinated anions have already been reported,[1–3] the gas permeation properties of SILMs containing fluorinated anions, such as those selected herein, have still not been properly studied and discussed. Only three studies have reported SILMs that made use of $[C_4F_9SO_3]^-$, $[FAP]^-$ and $[BETI]^-$ anions. Pereiro *et al.*[32] conducted single gas permeation experiments through a $[C_2C_1py][C_4F_9SO_3]$ SILM, at 294 K and 75 kPa, using CO_2, N_2, O_2, hydrocarbon gases (CH_4, C_2H_6, C_3H_8, C_3H_6) and perfluorocarbon gases (CF_4, C_2F_6, C_3F_8). Scovazzo *et al.*[22] determined ideal/mixed CO_2/CH_4 and CO_2/N_2 permselectivities in a $[C_4mim][BETI]$ SILM at 303 K and 200 kPa, while Althuluth *et al.*[33] reported ideal/mixed CO_2/CH_4 permselectivities in a $[C_2mim][FAP]$ SILM at 313 K and 700 kPa. Nevertheless, the obtained results cannot be directly compared due to the different measurement conditions, as well as the use of diverse IL cation structures.

Additionally, this work investigates the impact on gas transport through SILMs of using a pure IL *versus* a structurally similar IL mixture as the liquid phase. Inspired by the fact that the $[TFSAM]^-$ anion has an unusual asymmetric chemical structure, which combines both fluorinated and cyano functionalities, the re-design of the chemical structure of a pure $[C_2mim][TFSAM]$ IL through the use of IL mixtures is explored. For that purpose, different pairs of ILs, based on the $[C_2mim]^+$ cation and anions containing fluorinated or cyano functionalities, were selected and their gas permeation properties were compared to those of the pure $[C_2mim][TFSAM]$ SILM. One of the IL mixtures contains $[NTf_2]^-$ and $[N(CN)_2]^-$ anions, whose gas permeation properties were previously determined,[29] whereas the other IL mixture is based on $[OTf]^-$ and $[SCN]^-$ anions and its gas transport properties are reported here for the first time.

Results and discussion

Gas permeation through SILMs having fluorinated anions

The structures of the pure ILs bearing fluorinated anions are depicted in Fig. 1.

The water content (wt%), molar mass (M), viscosity (η), density (ρ) and molar volume (V_m) values of the pure ILs used as liquid phases in the studied SILMs are summarized in Table 1. The thermophysical properties of the conventional $[C_2mim][NTf_2]$ IL are also included for comparison.[29] From Table 1, it can be observed that the IL containing the $[C_4F_9SO_3]^-$ anion shows the highest viscosity, while $[C_2mim][FSI]$ presents the lowest viscosity. The IL viscosity values can be organized following the IL anion order: $[C_4F_9SO_3]^- > [BETI]^- > [FAP]^- > [NTf_2]^- > [TFSAM]^- > [FSI]^-$. A slightly different trend was observed for molar volumes, with the IL comprising the $[FAP]^-$ anion showing the highest molar volume, while $[C_2mim][FSI]$ exhibiting the lowest molar volume. These data will be used subsequently in the understanding of the gas permeation results.

The experimental gas permeability (P) values obtained through the prepared SILMs having ILs with fluorinated anions, measured at 293 K with a *trans*-membrane pressure differential of 100 kPa, are shown in Table 2. To the best of our knowledge, the CO_2/N_2 separation properties of $[C_2mim][TFSAM]$, $[C_2mim][FSI]$, $[C_2mim][FAP]$, $[C_2mim][BETI]$ and $[C_2mim][C_4F_9SO_3]$ SILMs are reported here for the first time, while those of the $[C_2mim][NTf_2]$ SILM were previously determined using the same experimental conditions.[29] It is important to mention that in order to attain stable SILMs, both hydrophilic and hydrophobic supports were used according to the hydrophobicity of ILs, and the results are compared in this section, irrespective of the support used.

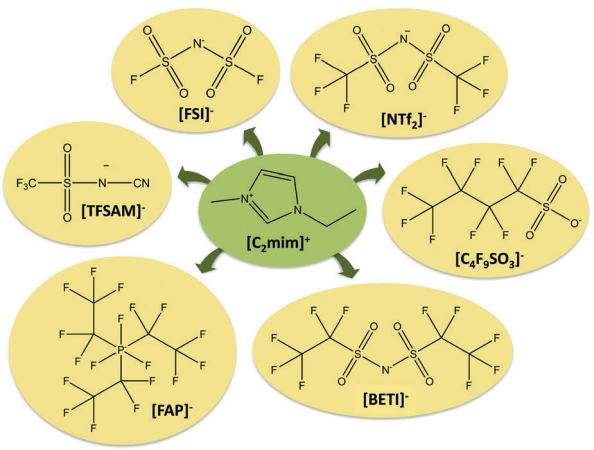

Fig. 1 Chemical structures of the pure ionic liquids (ILs) used in this work to prepare SILMs.

Table 1 Water contents and thermophysical properties of the pure ILs

IL sample	H_2O (wt%)	M (g mol^{-1})	η^a (mPa s)	ρ^b (g cm^{-3})	V_m (cm^3 mol^{-1})
[C_2mim][TFSAM]	0.02	284.26	23.7	1.3518	210.3
[C_2mim][FSI]	0.09	291.30	22.4	1.4480	201.2
[C_2mim][NTf_2]^c	0.02	391.31	39.1	1.5240	256.8
[C_2mim][FAP]^d	—	556.17	76.4	1.7081	325.6
[C_2mim][BETI]	0.02	491.33	85.5	1.5989	307.3
[C_2mim][$C_4F_9SO_3$]	0.08	410.26	109.7	1.5420	266.1

^{a} Viscosity (η) and density (ρ) measured at 293 K, except for [C_2mim][$C_4F_9SO_3$] IL (303 K). ^{b} Molar volume (V_m) obtained for 293 K, except for [C_2mim][$C_4F_9SO_3$] IL (303 K). ^{c} The values of [C_2mim][NTf_2] were taken from Tomé *et al.*[29] ^{d} The density and viscosity values of [C_2mim][FAP] were taken from Neves *et al.*[52]

Table 2 Gas permeabilities (P)^a through the prepared SILMs of pure ILs^b

SILM sample	P (CO_2)	P (N_2)	α (CO_2/N_2)
[C_2mim][TFSAM]	753 ± 0.2	17 ± 0.1	43.9 ± 0.1
[C_2mim][FSI]	843 ± 0.5	18 ± 0.2	46.1 ± 0.5
[C_2mim][NTf_2]^c	589 ± 1.0	17 ± 0.1	35.5 ± 0.3
[C_2mim][FAP]	624 ± 0.4	24 ± 0.1	26.0 ± 0.1
[C_2mim][BETI]	437 ± 1.9	18 ± 0.1	24.8 ± 0.2
[C_2mim][$C_4F_9SO_3$]	32 ± 0.2	6 ± 0.1	5.5 ± 0.1

^{a} Barrer (1 Barrer = 10^{-10} $cm_{(STP)}^3$ cm cm^{-2} s^{-1} cmHg^{-1}). ^{b} The listed uncertainties represent the standard deviations, based on three experiments. ^{c} Values taken from Tomé *et al.*[29]

From Table 2, the same trend in gas permeability is valid for all the studied SILMs: $PCO_2 \gg PN_2$, as expected. Regarding the influence of the fluorinated-based anions, SILMs having the $[FSI]^-$, $[TFSAM]^-$ and $[FAP]^-$ anions present higher CO_2 permeabilities of 843, 753 and 624 Barrer, respectively, than the SILM containing the $[NTf_2]^-$ anion, which is well-known for its high CO_2 permeability (589 Barrer).[29] It should be noted that in spite of the similar structures of $[NTf_2]^-$ and $[FSI]^-$ anions, in which the difference consists in two extra $^-CF_3$ groups in the $[NTf_2]^-$ anion structure (Fig. 1), the CO_2 permeability through the [C_2mim][FSI] SILM is ~1.5 times higher than that through the [C_2mim][NTf_2] SILM. Generally, CO_2 permeabilities through the studied SILMs are found to decrease in the following IL anion order: $[FSI]^- > [TFSAM]^- > [FAP]^- > [NTf_2]^- > [BETI]^- > [C_4F_9SO_3]^-$ (Table 2). Considering the IL anion viscosity trend, obtained at 293 K (Table 1), $[FSI]^- < [TFSAM]^- < [NTf_2]^- < [FAP]^- < [BETI]^- < [C_4F_9SO_3]^-$, it can be concluded that these experimental data are in agreement with the general trend usually observed in the literature, where ILs with high viscosities yield SILMs with low gas permeabilities.[3,14,15,23,40] However, [C_2mim][FAP] is the only exception since it presents a different behaviour (Table 2): despite its high viscosity (76.4 mPa s), it also exhibits high CO_2 permeability (624 Barrer), higher than those of the [C_2mim][NTf_2] IL (39.1 mPa s and 589 Barrer). Notice that the $[FAP]^-$ anion has the most different chemical structure among all the IL anions studied in this work, consisting of a phosphorus atom surrounded by fluorine atoms, without sulfonyl functional groups (Fig. 1). Moreover, taking a closer look at the gas permeabilities obtained through SILMs immobilized with the remaining ILs, it can be seen that higher CO_2 permeabilities are achieved for ILs with anions bearing a smaller number of fluorine elements, such as $[TFSAM]^-$ and $[FSI]^-$ anions (Table 2).

Gas diffusivity (D) is a mass transfer property that directly accounts for gas permeability (eqn (1)). Typically, the higher the gas diffusivity, the faster is the gas flux through the SILM. The experimental CO_2 and N_2 diffusivity values obtained through the prepared SILMs are presented in Table 3. The CO_2 diffusivities of the SILMs with fluorinated anions can be ordered as follows: $[FSI]^- > [TFSAM]^- > [FAP]^- > [NTf_2]^- > [BETI]^- > [C_4F_9SO_3]^-$, which fully corresponds to the IL anion order observed for CO_2 permeabilities (Table 2). As for N_2 diffusivities the subsequent order is attained: $([FAP]^- > [FSI]^- > [TFSAM]^- > [BETI]^- > [NTf_2]^- > [C_4F_9SO_3]^-)$, which is nearly the same IL anion order observed for N_2 permeabilities, but different from that obtained for CO_2 diffusivities and permeabilities.

The relationship between IL viscosity and gas diffusion is in fact the basis of the dependence of permeability on viscosity that we have shown above. A number of works have reported the inversely proportional relationship between gas diffusivity and IL viscosity.[3,16,17,41] Along this line of thought, the relationship between experimental CO_2 diffusivities and IL viscosity for the studied SILMs is depicted in Fig. 2.

In agreement to what was previously observed in the literature for other SILMs,[4,21–23] the CO_2 diffusivity through SILMs having fluorinated anions decreases as the IL viscosity increases. The SILMs with the lowest CO_2 diffusivities are [C_2mim][$C_4F_9SO_3$] (55×10^{-12} m^2 s^{-1}) and [C_2mim][BETI] (167×10^{-12} m^2 s^{-1}), which also have the lowest CO_2 permeabilities (437 and 32 Barrer), depicting the highest viscosities (109.7 and 85.5 mPa). Similarly to what is mentioned above for CO_2 permeabilities, again a deviant behaviour can be observed for the [C_2mim][FAP] SILM, since its CO_2 diffusivity is in between those of [C_2mim][NTf_2] and [C_2mim][TFSAM] (Table 3), but its viscosity values (76.4 mPa s) are higher than those of [C_2mim][NTf_2] (39.1 mPa s) and [C_2mim][TFSAM] (23.7 mPa s) (Fig. 2).

The gas solubility (S) values calculated using Eqn 1 are listed in Table 4. It can be seen that the [C_2mim][$C_4F_9SO_3$] SILM presents the lowest CO_2 solubility (4×10^{-6} $m_{(STP)}^3$ m^{-3} Pa^{-1}), while the previously reported [C_2mim][NTf_2] SILM has the highest CO_2 solubility (26×10^{-6} $m_{(STP)}^3$ m^{-3} Pa^{-1}). The CO_2 solubility values of the remaining studied SILMs having different fluorinated anions are very similar (ranging from 20×10^{-6}

Table 3 Gas diffusivity (D) values through the prepared SILMs of pure ILs

SILM sample	Gas diffusivity ($\times 10^{12}$) (m^2 s^{-1})	
	D (CO_2)	D (N_2)
[C_2mim][TFSAM]	258 ± 1.1	291 ± 4.5
[C_2mim][FSI]	315 ± 4.4	353 ± 7.5
[C_2mim][NTf_2]^a	172 ± 1.7	203 ± 2.5
[C_2mim][FAP]	214 ± 1.9	326 ± 0.2
[C_2mim][BETI]	167 ± 2.1	216 ± 2.4
[C_2mim][$C_4F_9SO_3$]	55 ± 1.2	88 ± 2.0

^{a} The gas diffusivity values through the [C_2mim][NTf_2] SILM were taken from Tomé *et al.*[29]

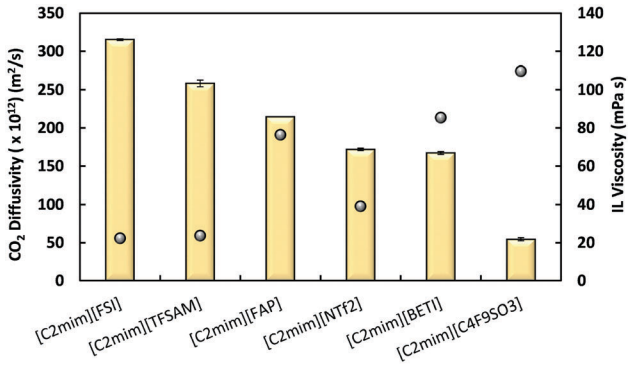

Fig. 2 Relationship between the CO_2 diffusivities determined through the SILMs prepared with pure ILs and the respective IL viscosities measured at 293 K. Error bars represent standard deviations based on three experimental replicas.

to 22 × 10^{-6} $m_{(STP)}^3$ m^{-3} Pa^{-1}) and can be ordered as follows: $[TFSAM]^-$ ≈ $[FAP]^-$ > $[FSI]^-$ ≈ $[BETI]^-$. Regarding the N_2 solubility, its values are always significantly lower (between 0.39 × 10^{-6} and 0.61 × 10^{-6} $m_{(STP)}^3$ m^{-3} Pa^{-1}) than those of CO_2 for all the SILMs studied.

Over the past few years, a number of correlations have been proposed with the intention of understanding the relationships between CO_2 solubility and the intrinsic properties of ILs.[42–44] The proposed models showed that CO_2 solubility increases with increasing IL molecular weight, molar volume and free volume.[10] Taking into consideration the gas solubility results obtained in this work (Table 4), as well as the range of molar volumes (from 201.2 up to 325.6 cm^3 mol^{-1}) and molecular weights (from 284.3 up to 556.2 g mol^{-1}) of the ILs used, divergences from the abovementioned trends can be found for the studied SILMs having fluorinated anions. For example, the $[C_2mim][NTf_2]$ SILM shows the highest CO_2 solubility (26 × 10^{-6} $m_{(STP)}^3$ m^{-3} Pa^{-1}), but it does not have the highest IL molar volume and molecular weight (Table 1). Likewise, the lowest CO_2 solubility (4 × 10^{-6} $m_{(STP)}^3$ m^{-3} Pa^{-1}) belongs to the $[C_2mim][C_4F_9SO_3]$ SILM, although it does not present the lowest IL molar volume and molecular weight (Table 1). The effect of fluorination, either in the IL cation or anion, on CO_2 solubility has been studied by different researchers.[19,45–47] Tagiuri *et al.*[48] explored the effect of cation on the CO_2 solubility of three different ILs combining the $[FSI]^-$ anion. Moreover, Kroon *et al.*[49] determined the CO_2 solubility in the $[C_2mim][FAP]$ IL by measuring the bubble point pressures of the binary mixture of $[C_2mim][FAP]$ + CO_2. The results showed that the CO_2 solubility in $[C_2mim][FAP]$ is higher when compared to that of ILs having the same cation combined with other fluorinated anions such as $[NTf_2]^-$, $[BF_4]^-$ and $[PF_6]^-$, due to the fact that $[FAP]^-$ has a large size and it is highly fluorinated. Although it has been recognized that introducing fluorination into the cation and/or anion can effectively improve CO_2 solubility,[46] it was recently reported after critical analysis that no special effect of the fluorination upon the CO_2 solubility has been observed for both perfluorocarbon and heavily fluorinated ILs.[50] In fact, the introduction of fluorination into the anions of the ILs studied in this work does not significantly affect the obtained gas solubility values (Table 4), except for the case of the $[C_2mim][C_4F_9SO_3]$ IL that displays a very low CO_2 solubility.

Table 4 Gas solubility (*S*) values through the prepared SILMs of pure ILs

	Gas solubility (×10^6) ($m_{(STP)}^3$ m^{-3} Pa^{-1})	
SILM sample	*S* (CO_2)	*S* (N_2)
$[C_2mim][TFSAM]$	22 ± 0.09	0.44 ± 0.01
$[C_2mim][FSI]$	20 ± 0.29	0.39 ± 0.01
$[C_2mim][NTf_2]$[a]	26 ± 0.28	0.61 ± 0.01
$[C_2mim][FAP]$	22 ± 0.21	0.55 ± 0.001
$[C_2mim][BETI]$	20 ± 0.17	0.61 ± 0.01
$[C_2mim][C_4F_9SO_3]$	4 ± 0.07	0.49 ± 0.002

[a] The gas solubility values through the $[C_2mim][NTf_2]$ SILM were taken from Tomé *et al.*[29]

Re-designing the $[TFSAM]^-$ anion by structural unfolding: effect on gas permeation

Taking into account that the $[TFSAM]^-$ anion has an unconventional and asymmetric chemical structure, combining both fluorinated and cyano functionalities, which have both been recognized to be responsible for high CO_2 separation performance, we explore here the effect of structural unfolding of the pure $[C_2mim][TFSAM]$ IL on gas permeation properties of SILMs using IL mixtures. Thus, two equimolar IL mixtures were used for this purpose: $[C_2mim][SCN][OTf]$ (Fig. 3), which is studied here for the first time, and $[C_2mim][N(CN)_2][NTf_2]$, whose gas permeation and thermophysical properties were previously determined by us.[29] Both these mixtures have IL anions that show structural similarities to the $[TFSAM]^-$ anion (Fig. 3). The composition description, water content (wt%), molar mass (M), viscosity (η), density (ρ) and molar volume (V_m) values of the pure ILs, $[C_2mim][TFSAM]$, $[C_2mim][SCN]$, $[C_2mim][OTf]$, $[C_2mim][N(CN)_2]$, $[C_2mim][NTf_2]$, and the selected IL mixtures are listed in Table 5, while their gas permeability, diffusivity and solubility values are depicted in Fig. 4(a)–(c), respectively.

Fig. 4(a) and (b) show that the pure $[C_2mim][TFSAM]$ SILM exhibits higher gas permeabilities and diffusivities than SILMs

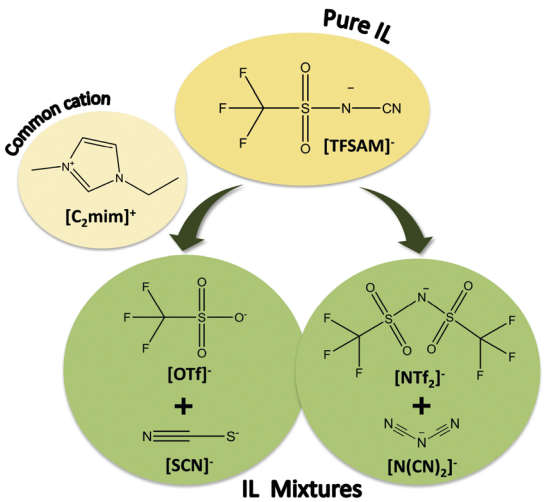

Fig. 3 Chemical structures of the pure IL and IL mixtures studied in this work.

Table 5 Composition descriptions, water contents and thermophysical properties of the pure ILs and IL mixtures

IL sample	Composition description (mole fraction)	H_2O (wt%)	M (g mol^{-1})	η^a (mPa s)	ρ^b (g cm^{-3})	V_m (cm^3 mol^{-1})
[C_2mim][TFSAM]	Pure	0.02	284.26	23.7	1.3518	210.3
[C_2mim][SCN][c]	Pure	0.09	169.25	27.9	1.1190	151.2
[C_2mim][SCN][OTf]	0.5 [C_2mim][SCN] + 0.5 [C_2mim][OTf]	0.16	214.74	36.4	1.2638	169.9
[C_2mim][OTf]	Pure	0.10	260.23	49.5	1.3850	187.9
[C_2mim][N(CN)$_2$][c]	Pure	0.09	177.21	18.0	1.1060	160.2
[C_2mim][N(CN)$_2$][NTf$_2$][c]	0.5[C_2mim][N(CN)$_2$] + 0.5 [C_2mim][NTf$_2$]	0.12	284.26	29.2	1.3620	208.7
[C_2mim][NTf$_2$][c]	Pure	0.02	391.31	39.1	1.5240	256.8

[a] Viscosity (η) and density (ρ) measured at 293 K. [b] Molar volume (V_m) obtained at 293 K. [c] The values of [C_2mim][N(CN)$_2$][NTf$_2$] were taken from Tomé *et al.*[29]

composed of both [C_2mim][SCN][OTf] and [C_2mim][N(CN)$_2$][NTf$_2$] IL mixtures. Moreover, the addition of 0.5 mole fraction of [C_2mim][SCN] did not significantly affect CO_2 permeability but decreased to almost half the N_2 permeability compared to those of the pure [C_2mim][OTf] SILM. From Fig. 4(b), where the relationship between CO_2 diffusivity and IL viscosity is illustrated, it can also be seen that both [C_2mim][N(CN)$_2$][NTf$_2$] and [C_2mim][SCN][OTf] IL mixtures present slightly higher viscosities (Table 5) and lower CO_2 diffusivities than those of the pure [C_2mim][TFSAM] SILM. Also, the presence of 0.5 mole fraction of [C_2mim][SCN] leads to a decrease in IL viscosity and an increase in CO_2 diffusivity. The same behaviour was found for [C_2mim][N(CN)$_2$][NTf$_2$] with the addition of 0.5 mole fraction of [C_2mim][N(CN)$_2$]. These results are in accordance with the general trend observed in the literature: the CO_2 diffusivity decreases with the increase in IL viscosity.[4,21–23]

Concerning gas solubility, from Fig. 4(c), it can be observed that CO_2 solubilities of both IL mixtures are in between those of the individual IL components. Moreover, the presence of 0.5 mole fraction of [C_2mim][OTf] or [C_2mim][NTf$_2$] in the corresponding mixtures leads to an increase in the CO_2 solubilities, probably due to the fact that they present higher molar volume compared to the pure [C_2mim][SCN] or [C_2mim][N(CN)$_2$], respectively. Furthermore, the [C_2mim][N(CN)$_2$][NTf$_2$] mixture displays a CO_2 solubility (20×10^{-6} $m_{(STP)}^3$ m^{-3} Pa^{-1}) closer to that of the pure [C_2mim][TFSAM] SILM (22×10^{-6} $m_{(STP)}^3$ m^{-3} Pa^{-1}), probably due to the fact that these IL phases have very close molar volumes (208.7 and 210.3 cm^3 mol^{-1}, respectively) and the same molecular weight (284.3 g mol^{-1}). Conversely, the [C_2mim][SCN][OTf] mixture has lower CO_2 solubility (15×10^{-6} $m_{(STP)}^3$ m^{-3} Pa^{-1}) than that observed for the pure [C_2mim][TFSAM] SILM, which is in agreement with the lower molar volume (169.9 cm^3 mol^{-1}) and molecular weight (214.7 cm^3 mol^{-1}) presented by this IL mixture containing the [SCN]$^-$ and [OTf]$^-$ anions. Despite the fact that it is possible to obtain similar viscosities and molar volumes of the pure [C_2mim][TFSAM] IL by mixing the [C_2mim][N(CN)$_2$] and [C_2mim][NTf$_2$] ILs, improved gas permeabilities, diffusivities and solubilities were obtained through the pure [C_2mim][TFSAM] SILM.

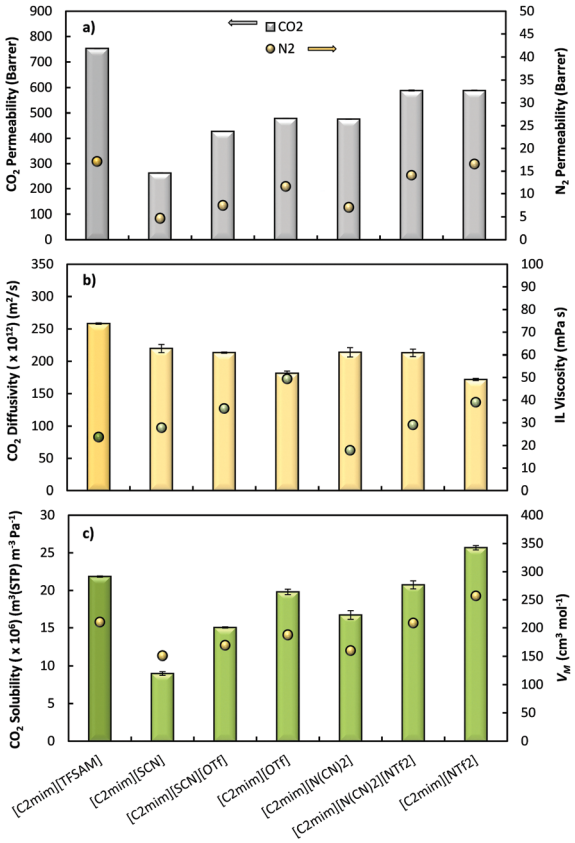

Fig. 4 (a) Gas permeability, (b) CO_2 diffusivity as a function of IL viscosity and (c) CO_2 solubility as a function of IL molar volume for the studied SILMs. Error bars represent standard deviations based on three experimental replicas. The gas permeability, diffusivity and solubility values of [C_2mim][N(CN)$_2$][NTf$_2$] and [C_2mim][NTf$_2$] were taken from Tomé *et al.*[29]

Comparison of CO_2/N_2 separation performance

The gas permeabilities and CO_2/N_2 permselectivities of all the studied SILMs are listed in Table 6. Amongst the pure SILMs with fluorinated anions, the [C_2mim][FSI] and [C_2mim][TFSAM] SILMs not only show the highest gas permeabilities (843 and 753 Barrer, respectively), but also have the largest CO_2/N_2 permselectivities (43.9 and 46.1, respectively). In contrast, the lowest gas permeabilities and CO_2/N_2 permselectivity belong to the [C_2mim][$C_4F_9SO_3$] SILM. The CO_2/N_2 permselectivities of the pure SILMs decrease as the fluorinated chain increases in the IL anion: [FSI]$^-$ > [TFSAM]$^-$ > [NTf$_2$]$^-$ > [BETI]$^-$, the [C_2mim][FAP] and [C_2mim][$C_4F_9SO_3$] SILMs being the only exceptions.

Concerning the effect of the structural unfolding of the [TFSAM]$^-$ anion, and as previously discussed, the pure [C_2mim][TFSAM] SILM presents higher gas permeabilities compared to its structurally similar IL mixtures (Table 6). Nevertheless, the greatest CO_2/N_2

Table 6 Single gas permeability (P)[a] and ideal permselectivities (α) of all the studied SILMs[b]

SILM sample	P (CO_2)	P (N_2)	α (CO_2/N_2)
[C_2mim][TFSAM]	753 ± 0.2	17 ± 0.1	43.9 ± 0.1
[C_2mim][FSI]	843 ± 0.5	18 ± 0.2	46.1 ± 0.5
[C_2mim][FAP]	624 ± 0.4	24 ± 0.1	26.0 ± 0.1
[C_2mim][BETI]	437 ± 1.9	18 ± 0.1	24.8 ± 0.2
[C_2mim][$C_4F_9SO_3$]	32 ± 0.2	6 ± 0.1	5.5 ± 0.1
[C_2mim][SCN][c]	263 ± 0.6	5 ± 0.2	56.6 ± 1.9
[C_2mim][SCN][OTf]	428 ± 0.5	7 ± 0.1	57.6 ± 0.4
[C_2mim][OTf]	479 ± 0.6	12 ± 0.1	41.4 ± 0.3
[C_2mim][$N(CN)_2$][c]	476 ± 0.8	7 ± 0.1	67.8 ± 0.6
[C_2mim][$N(CN)_2$][NTf_2][c]	589 ± 1.9	14 ± 0.2	41.8 ± 0.7
[C_2mim][NTf_2][c]	589 ± 1.0	17 ± 0.1	35.5 ± 0.3

[a] Barrer (1 Barrer = 10^{-10} $cm_{(STP)}^3$ cm cm^{-2} s^{-1} $cmHg^{-1}$). [b] The listed uncertainties represent the standard deviations, based on three experiments. [c] Values taken from Tomé *et al.*[29]

permselectivity (57.6) was achieved for the SILM containing the [C_2mim][SCN][OTf] IL mixture.

With the purpose of comparing the performance results obtained in this work to those reported in the literature for other SILMs, Fig. 5 displays the Robeson plot for CO_2/N_2 separation, where the CO_2/N_2 permselectivity is plotted against CO_2 permeability and the solid black line represents the empirical 2008 upper bound for this gas pair.[51] It can be seen that among the SILMs immobilized with the pure IL having fluorinated anions, both the [C_2mim][TFSAM] and [C_2mim][FSI] SILMs fall or exceed the Robeson 2008 upper bound, meaning that these two ILs are the most promising candidates for CO_2/N_2 separation processes. Comparing the results of the pure [C_2mim][TFSAM] SILM with those of selected IL mixtures, Fig. 5 clearly shows that the CO_2/N_2 separation performance of the SILM immobilized with the [C_2mim][SCN][OTf] IL mixture surpasses the upper bound, primarily due to its higher CO_2/N_2 permselectivity (57.6). On the other hand, the CO_2/N_2 separation efficiency of the [C_2mim][$N(CN)_2$][NTf_2] SILM is on top of the upper bound, since it presents lower permselectivity (41.8), despite its high CO_2 permeability (589 Barrer) in comparison to that of the [C_2mim][SCN][OTf] SILM (428 Barrer). Actually, it is the [C_2mim][$N(CN)_2$][NTf_2] SILM that discloses the most similar CO_2/N_2 separation performance results to the pure synthesized [C_2mim][TFSAM] IL (Fig. 5).

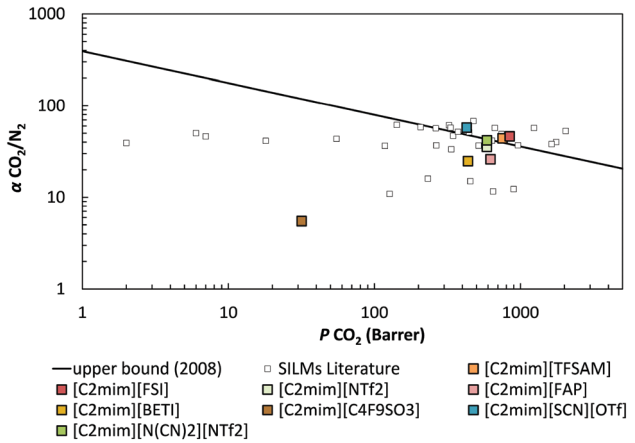

Fig. 5 CO_2/N_2 separation performance of all the studied SILMs. The experimental error is within the data points. Data are plotted on a log–log scale and the upper bound is adapted from Robeson.[51] The literature data previously reported for other SILMs (□)[15,17,22,24,29,30,32,53] are also illustrated for comparison. The values of [C_2mim][$N(CN)_2$][NTf_2] and [C_2mim][NTf_2] SILMs were taken from Tomé *et al.*[29]

Experimental

Materials

Lithium bis(pentafluoroethylsulfonyl)imide ($Li(CF_3CF_2SO_2)_2N$, LiBETI, 98%, Chameleon Reagent) and lithium nonafluoro-1-butanesulfonate ($LiC_4F_9SO_3$, > 95%, TCI Chemicals) were used without purification. Reagent-grade dichloromethane, acetonitrile, hexane and ethyl acetate were obtained from Aldrich or Merck and were dried by vacuum distillation over P_2O_5. *N*-Methylimidazole (98%, Aldrich) and bromoethane (98%, Acros) were distilled under an inert atmosphere over CaH_2.

1-Ethyl-3-methylimidazolium bis(fluorosulfonyl)imide ([C_2mim][FSI], 99.5 wt%, Solvionic), 1-ethyl-3-methylimidazolium tris(pentafluoro-ethyl)trifluorophosphate ([C_2mim][FAP], 98 wt%, Merck), 1-ethyl-3-methylimidazolium thiocyanate ([C_2mim][SCN], > 98 wt%, IoLiTec) and 1-ethyl-3-methylimidazolium trifluoromethanesulfonate ([C_2mim][OTf], ≥ 98 wt%, Aldrich) were obtained from the specified suppliers. To reduce the content of water and other volatile substances, the pure ILs were dried at approximately 1 Pa and 318 K for at least 4 days.

IL synthesis and characterization

1-Ethyl-3-methylimidazolium bromide ([C_2mim][Br]). [C_2mim][Br] was synthesized by the reaction between *N*-methylimidazole and an excess of bromoethane following the method used in a previous work.[34] Spectroscopic data of the target compound were in accordance with those reported in the literature.

1-Ethyl-3-methylimidazolium 2,2,2-trifluoromethylsulfonyl-*N*-cyanoamide ([C_2mim][TFSAM]). [C_2mim][TFSAM] was prepared by ion exchange between [C_2mim][Br] and KTFSAM, in an aqueous medium in accordance with a described procedure.[35] Yield: 85%; anal. calcd for $C_8H_{11}N_4F_3SO_2$ (284.26), %: N, 19.71%; C, 33.80%; H, 3.90%; Found, %: N, 19.68%; C, 33.78%; H, 3.99%; ^{1}H NMR (300 MHz, DMSO-d_6): 9.08 (s, 1H, 2H (Im)), 7.72 (s, 1H, H4 (Im)), 7.64 (s, 1H, H5 (Im)), 4.22–4.15 (m, 2H, $\underline{CH_2}CH_3$), 3.84 (s, 3H, CH_3), 1.42 (t, 3H, $CH_2\underline{CH_3}$, J_{HH} = 7.5 Hz); ^{13}C NMR (100.6 MHz, DMSO-d_6): 136.1, 125.0–115.4 (q, $^1J_{CF}$ = 325 Hz), 123.4, 121.8, 44.1, 35.5, 14.8; ^{19}F NMR (282.4 MHz, DMSO-d_6): −77.8; IR (KBr pellet): 3158 (m, ν_{C-H}), 3117 (m, ν_{C-H}), 2192 (vs, ν_{C-N}), 1573 (m), 1468 (w), 1333 (vs, ν_{asSO_2}), 1236 (s), 1217 (vs, ν_{CF}), 1170 (vs, ν_{sSO_2}), 1119 (s, ν_{CF}), 832 (s), 752 (w), 639 (m), 595 (s), 479 (m) cm^{-1}.

1-Ethyl-3-methylimidazolium nonafluorobutanesulfonate ([C_2mim][$C_4F_9SO_3$]). Lithium nonafluoro-1-butanesulfonate (8.00 g, 0.026 mol) was dissolved in 20 mL of distilled water and added dropwise to a solution of [C_2mim][Br] (3.84 g, 0.020 mol) in 15 mL of H_2O at ambient temperature. The solution was stirred for 2 h at room temperature and then [C_2mim][$C_4F_9SO_3$] was extracted

with dichloromethane (4 × 40 mL). The combined CH_2Cl_2 solution was washed with a small amount of water and dried over anhydrous $MgSO_4$. The magnesium sulfate was filtered off and dichloromethane was stripped off under reduced pressure. The product was obtained as slightly yellow transparent fluid oil, which was finally dried at 323 K and 100 Pa for 12 h using a special flask filled with P_2O_5 and introduced into the vacuum line. Yield: 5.61 g (68%); anal. calcd for $C_{10}H_{11}N_2F_9SO_3$ (410.26), %: C, 29.28%; H, 2.70%; F, 41.68%; Found, %: C, 28.99%; H, 2.83%; F, 41.39%; ^{1}H NMR (300 MHz, DMSO-d_6): 9.09 (s, 1H, H2 (Im)), 7.77 (s, 1H, H4 (Im)), 7.68 (s, 1H, H5 (Im)), 4.22–4.17 (m, 2H, $\underline{CH_2}CH_3$), 3.85 (s, 3H, CH_3), 1.43–1.39 (m, 3H, $CH_2\underline{CH_3}$); ^{13}C NMR (100.6 MHz, DMSO-d_6): 136.2, 123.5, 121.9, 117.1 (qt, $-CF_2-\underline{C}F_3$, ^1J = 288 Hz, ^2J = 34 Hz), 113.4 (tt, $(-)O_3S-\underline{C}F_2-$, ^1J = 288 Hz, ^2J = 34 Hz), 110.4 (tp, $(-)O_3S-CF_2-\underline{C}F_2-$, ^1J = 266, ^2J = 33 Hz), 109.8 (qq, $-\underline{C}F_2-CF_3$, ^1J = 268 Hz, ^2J = 38 Hz), 44.1, 35.6, 14.9; ^{19}F NMR (282.4 MHz, DMSO-d_6): −80.8, −114.9, −121.6, −125.9; IR (KBr pellet): 3156 (s, ν_{C-H}), 3117 (s, ν_{C-H}), 2993 (m, ν_{C-H}), 1574 (s), 1462 (m), 1432 (w), 1393 (w), 1353 (s), 1261 (vs, ν_{asSO_2}), 1236 (vs), 1214 (vs, ν_{CF}), 1170 (vs, ν_{sSO_2}), 1134 (s, ν_{CF}), 1057 (vs), 1119 (m), 1006 (m), 988 (w), 870 (m), 845 (m), 802 (m), 736 (m), 699 (m), 679 (w), 656 (s), 620 (s), 596 (m), 564 (m), 532 (s) cm^{-1}.

1-Ethyl-3-methylimidazolium bis(pentafluoroethylsulfonyl)imide ([C_2mim][BETI]). The procedure previously described for [C_2mim][$C_4F_9SO_3$] was also used for the synthesis of [C_2mim][BETI]. After purification and drying, [C_2mim][BETI] was obtained as colorless transparent fluid liquid. Yield: 82%; anal. calcd for $C_{10}H_{11}N_3F_{10}S_2O_4$ (491.32), %: C, 24.45%; H, 2.26%; N, 8.55%; Found, %: C, 24.50%; H, 2.03%; N, 8.49%; ^{1}H NMR (300 MHz, DMSO-d_6): 9.11 (s, 1H, H2 (Im)), 7.76 (s, 1H, H4 (Im)), 7.68 (s, 1H, H5 (Im)), 4.22–4.16 (m, 2H, $\underline{CH_2}CH_3$), 3.84 (s, 3H, CH_3), 1.43–1.40 (m, 3H, $CH_2\underline{CH_3}$); ^{13}C NMR (100.6 MHz, DMSO-d_6): 136.7, 123.9, 122.4, 117.7 (qt, $-CF_2-\underline{C}F_3$, ^1J = 287 Hz, ^2J = 34 Hz), 110.1 (tq, $-\underline{C}F_2-CF_3$, ^1J = 293 Hz, ^2J = 37 Hz), 44.6, 36.0, 15.4; ^{19}F NMR (282.4 MHz, DMSO-d_6): −78.8, −117.6; IR (KBr pellet): 3160 (m, ν_{C-H}), 3124 (m, ν_{C-H}), 2993 (w, ν_{C-H}), 1574 (m), 1472 (w), 1432 (w), 1355 (vs, ν_{asSO_2}), 1331 (vs, ν_{CF}), 1223 (vs, ν_{CF}), 1172 (vs, ν_{sSO_2}), 1087 (s, ν_{CF}), 978 (s), 824 (w), 775 (w), 755 (m), 742 (m), 701 (w), 644 (m), 616 (s), 536 (m), 525 (m) cm^{-1}.

NMR spectra were recorded on an AMX-400 spectrometer (Bruker) at 298 K in the indicated deuterated solvent and are listed in ppm. The signal corresponding to the residual protons of the deuterated solvent was used as an internal standard for ^{1}H and ^{13}C NMR, while for ^{19}F NMR $CHCl_2F$ was used as an external standard. IR spectra were acquired on a Nicolet Magna-750 Fourier IR-spectrometer using KBr pellets (128 scans, resolution was 2 cm^{-1}).

IL mixture preparation. The IL mixture, [C_2mim][SCN][OTf], containing 0.5 mole fraction of both [C_2mim][OTf] and [C_2mim][SCN], was prepared using an analytical high precision balance with an uncertainty of $\pm 10^{-5}$ g by syringing known masses of the IL components into a glass vial. Good mixing was ensured by magnetic stirring for 30 min at 298 K. Then, the IL mixture was dried at roughly 1 Pa and 318 K for at least 4 days immediately prior to use. The water contents of all IL samples were determined by Karl Fischer titration using a 831 KF Coulometer (Metrohm).

Density and viscosity determination. The density and viscosity measurements of the pure ILs and the [C_2mim][SCN][OTf] IL mixture were performed at 293 K and atmospheric pressure using an SVM 3000 Anton Paar rotational Stabinger viscometer-densimeter, where the standard uncertainty for the temperature was 0.02 K. The repeatability of density and dynamic viscosity of this equipment was 0.0005 g cm^{-3} and 0.35%, respectively. Measurements of each sample were performed in triplicate to ensure accuracy and the reported results are average values. The highest relative standard uncertainty registered for the density and dynamic viscosity measurements was 1×10^{-4} and 0.03, respectively.

Gas permeation measurements. Porous hydrophobic poly(vinylidene fluoride) (PVDF) membranes supplied by Millipore Corporation (USA), with a pore size of 0.22 μm and an average thickness of 125 μm, were used to support [C_2mim][FSI], [C_2mim][FAP] and [C_2mim][BETI]. Since the impregnation of the remaining IL samples into hydrophobic PVDF resulted in unstable SILMs, the other IL samples were supported on porous hydrophilic poly(tetrafluoroethylene) (PTFE) membranes acquired from Merck Millipore, with a pore size of 0.2 μm and an average thickness of 65 μm. All the SILM configurations were prepared by the vacuum method.[29]

Ideal gas permeabilities and diffusivities through the prepared SILMs were measured using a time-lag apparatus.[36] First, each SILM was degassed under vacuum inside the permeation cell for 12 h. Then, CO_2 and N_2 permeation experiments were carried out at 293 K with a *trans*-membrane pressure differential of 100 kPa. All the permeation data were measured at least in triplicate on a single SILM sample. The highest relative standard uncertainty registered for gas permeability measurements was 0.03. The permeation cell and lines were evacuated until the pressure was below 0.1 kPa before each run. No residual IL was found inside the permeation cell at the end of the experiments. The thickness of the SILMs was assumed to be equivalent to the membrane filter thickness.

Gas transport through the prepared SILMs was assumed to follow a solution–diffusion mass transfer mechanism,[37] where the permeability (P) is related to diffusivity (D) and solubility (S) as follows:

$$P = D \times S \tag{1}$$

The permeate flux of each gas (J_i) was determined experimentally using eqn (2),[38] where V^p is the permeate volume, Δp_d is the variation of downstream pressure, A is the effective membrane surface area, t is the experimental time, R is the gas constant and T is the temperature.

$$J_i = \frac{V^p \Delta p_d}{AtRT} \tag{2}$$

Ideal gas permeability (P_i) was then determined from the steady-state gas flux (J_i), the membrane thickness (ℓ) and the trans-membrane pressure difference (Δp_i), as shown in eqn (3).[38]

$$P_i = \frac{J_i}{\Delta p_i / \ell} \tag{3}$$

Gas diffusivity (D_i) was determined according to eqn (4). The time-lag parameter (θ) was calculated by extrapolating the slope of the linear portion of the p_d *vs.* t curve back to the time axis, where the intercept was equal to θ.[39]

$$D_i = \frac{\ell^2}{6\theta} \quad (4)$$

After P_i and D_i were known, the gas solubility (S_i) was calculated using the relationship shown in eqn (1). The ideal permeability selectivity (or permselectivity), $\alpha_{i/j}$, was obtained by dividing the permeability of the more permeable species i to the permeability of the less permeable species j. The permselectivity can also be expressed as the product of the diffusivity selectivity and the solubility selectivity:

$$\alpha_{i/j} = \frac{P_i}{P_j} = \left(\frac{D_i}{D_j}\right) \times \left(\frac{S_i}{S_j}\right) \quad (5)$$

Conclusions

In this work, ILs containing a common cation ($[C_2mim]^+$) and different fluorinated anions ($[TFSAM]^-$, $[FSI]^-$, $[C_4F_9SO_3]^-$, $[BETI]^-$, $[FAP]^-$) were synthesized and used as liquid phases to prepare SILMs for flue gas separation (CO_2/N_2). The single CO_2 and N_2 permeation properties through the prepared SILMs were determined. The viscosity and density of the IL phases were also evaluated. The results showed that CO_2 permeabilities and diffusivities through the studied SILMs follow the same fluorinated anion order: $[FSI]^- > [TFSAM]^- > [FAP]^- > [NTf_2]^- > [BETI]^- > [C_4F_9SO_3]^-$, which is inversely related to IL viscosity, with the only outlier being $[C_2mim][FAP]$. Conversely, the introduction of fluorination in the IL anions did not significantly affect gas solubility, except for the case of the $[C_2mim][C_4F_9SO_3]$ SILM displaying a very low CO_2 solubility. Among the pure SILMs, it is worth noting that the best separation performances were achieved for $[C_2mim][TFSAM]$ and $[C_2mim][FSI]$ SILMs that fall on top of or surpassed the Robeson 2008 upper bound, with CO_2 permeabilities of 753 and 843 Barrer and CO_2/N_2 permselectivities of 43.9 and 46.1, respectively.

Furthermore, the effect of structural unfolding of the $[TFSAM]^-$ anion on gas permeation properties of SILMs was investigated using IL mixtures comprising both fluorinated and cyano functionalities in the anions. The pure $[C_2mim][TFSAM]$ IL provided a membrane with improved CO_2 permeabilities, diffusivities and solubilities compared to those of the SILMs based on the selected $[C_2mim][SCN][OTf]$ and $[C_2mim][N(CN)_2][NTf_2]$ IL mixtures. Overall, and despite the fact that the $[C_2mim][SCN][OTf]$ SILM revealed better CO_2/N_2 separation performance essentially due to its higher CO_2/N_2 permselectivity (57.6), the $[C_2mim][N(CN)_2][NTf_2]$ IL mixture disclosed the most similar results to the pure synthesized $[C_2mim][TFSAM]$ IL, not only in terms of thermophysical properties, but also regarding gas transport and CO_2/N_2 separation performance.

Conflicts of interest

There are no conflicts to declare.

Acknowledgements

Andreia S. L. Gouveia and Liliana C. Tomé are grateful to FCT (Fundação para a Ciência e a Tecnologia) for their Doctoral (SFRH/BD/116600/2016) and Post-doctoral research grants (SFRH/BPD/101793/2014), respectively, Isabel M. Marrucho acknowledges FCT/MCTES (Portugal) for a contract under Investigador FCT 2012. This work was partially supported by FCT through the project PTDC/CTM-POL/2676/2014, R&D unit UID/Multi/04551/2013 (GreenIT), R&D unit UID/QUI/00100/2013 (CQE) and through the grant of President of the Russian Federation ''For Young Outstanding Professors'' (project no. MD-2371.2017.3).

Notes and references

1 L. C. Tomé and I. M. Marrucho, *Chem. Soc. Rev.*, 2016, **45**, 2785–2824.
2 Z. Dai, R. D. Noble, D. L. Gin, X. Zhang and L. Deng, *J. Membr. Sci.*, 2016, **497**, 1–20.
3 P. Scovazzo, *J. Membr. Sci.*, 2009, **343**, 199–211.
4 P. K. Parhi, *J. Chem.*, 2013, 11.
5 L. J. Lozano, C. Godínez, A. P. de los Ríos, F. J. Hernández-Fernández, S. Sánchez-Segado and F. J. Alguacil, *J. Membr. Sci.*, 2011, **376**, 1–14.
6 P. Luis, T. Van Gerven and B. Van der Bruggen, *Prog. Energy Combust. Sci.*, 2012, **38**, 419–448.
7 M. J. Earle, J. M. S. S. Esperanca, M. A. Gilea, J. N. Canongia Lopes, L. P. N. Rebelo, J. W. Magee, K. R. Seddon and J. A. Widegren, *Nature*, 2006, **439**, 831–834.
8 C. Cadena, J. L. Anthony, J. K. Shah, T. I. Morrow, J. F. Brennecke and E. J. Maginn, *J. Am. Chem. Soc.*, 2004, **126**, 5300–5308.
9 M. Hasib-ur-Rahman, M. Siaj and F. Larachi, *Chem. Eng. Process.*, 2010, **49**, 313–322.
10 M. Ramdin, T. W. de Loos and T. J. H. Vlugt, *Ind. Eng. Chem. Res.*, 2012, **51**, 8149–8177.
11 L. A. Neves, J. G. Crespo and I. M. Coelhoso, *J. Membr. Sci.*, 2010, **357**, 160–170.
12 P. C. Hillesheim, J. A. Singh, S. M. Mahurin, P. F. Fulvio, Y. Oyola, X. Zhu, D.-e. Jiang and S. Dai, *RSC Adv.*, 2013, **3**, 3981–3989.
13 P. C. Hillesheim, S. M. Mahurin, P. F. Fulvio, J. S. Yeary, Y. Oyola, D.-e. Jiang and S. Dai, *Ind. Eng. Chem. Res.*, 2012, **51**, 11530–11537.
14 S. M. Mahurin, T. Dai, J. S. Yeary, H. Luo and S. Dai, *Ind. Eng. Chem. Res.*, 2011, **50**, 14061–14069.
15 L. C. Tomé, D. J. S. Patinha, R. Ferreira, H. Garcia, C. Silva Pereira, C. S. R. Freire, L. P. N. Rebelo and I. M. Marrucho, *ChemSusChem*, 2014, **7**, 110–113.
16 R. Condemarin and P. Scovazzo, *Chem. Eng. J.*, 2009, **147**, 51–57.
17 L. Ferguson and P. Scovazzo, *Ind. Eng. Chem. Res.*, 2007, **46**, 1369–1374.
18 J. J. Close, K. Farmer, S. S. Moganty and R. E. Baltus, *J. Membr. Sci.*, 2012, **390–391**, 201–210.
19 J. E. Bara, C. J. Gabriel, T. K. Carlisle, D. E. Camper, A. Finotello, D. L. Gin and R. D. Noble, *Chem. Eng. J.*, 2009, **147**, 43–50.

20 P. Cserjési, N. Nemestóthy, A. Vass, Z. Csanádi and K. Bélafi-Bakó, *Desalination*, 2009, **245**, 743–747.
21 C. Myers, H. Pennline, D. Luebke, J. Ilconich, J. K. Dixon, E. J. Maginn and J. F. Brennecke, *J. Membr. Sci.*, 2008, **322**, 28–31.
22 P. Scovazzo, D. Havard, M. McShea, S. Mixon and D. Morgan, *J. Membr. Sci.*, 2009, **327**, 41–48.
23 S. M. Mahurin, J. S. Lee, G. A. Baker, H. Luo and S. Dai, *J. Membr. Sci.*, 2010, **353**, 177–183.
24 S. M. Mahurin, P. C. Hillesheim, J. S. Yeary, D.-e. Jiang and S. Dai, *RSC Adv.*, 2012, **2**, 11813–11819.
25 S. M. Mahurin, J. S. Yeary, S. N. Baker, D.-e. Jiang, S. Dai and G. A. Baker, *J. Membr. Sci.*, 2012, **401–402**, 61–67.
26 E. Kamio, T. Matsuki, S. Kasahara and H. Matsuyama, *Sep. Sci. Technol.*, 2017, **52**, 209–220.
27 S. Kasahara, E. Kamio, T. Ishigami and H. Matsuyama, *J. Membr. Sci.*, 2012, **415–416**, 168–175.
28 S. Kasahara, E. Kamio, T. Ishigami and H. Matsuyama, *Chem. Commun.*, 2012, **48**, 6903–6905.
29 L. C. Tomé, D. J. S. Patinha, C. S. R. Freire, L. P. N. Rebelo and I. M. Marrucho, *RSC Adv.*, 2013, **3**, 12220–12229.
30 L. C. Tomé, C. Florindo, C. S. R. Freire, L. P. N. Rebelo and I. M. Marrucho, *Phys. Chem. Chem. Phys.*, 2014, **16**, 17172–17182.
31 A. S. L. Gouveia, L. C. Tomé and I. M. Marrucho, *J. Membr. Sci.*, 2016, **510**, 174–181.
32 A. B. Pereiro, L. C. Tomé, S. Martinho, L. P. N. Rebelo and I. M. Marrucho, *Ind. Eng. Chem. Res.*, 2013, **52**, 4994–5001.
33 M. Althuluth, J. P. Overbeek, H. J. van Wees, L. F. Zubeir, W. G. Haije, A. Berrouk, C. J. Peters and M. C. Kroon, *J. Membr. Sci.*, 2015, **484**, 80–86.
34 Y. U. Paulechka, G. J. Kabo, A. V. Blokhin, A. S. Shaplov, E. I. Lozinskaya and Y. S. Vygodskii, *J. Chem. Thermodyn.*, 2007, **39**, 158–166.
35 A. S. Shaplov, E. I. Lozinskaya, P. S. Vlasov, S. M. Morozova, D. Y. Antonov, P. H. Aubert, M. Armand and Y. S. Vygodskii, *Electrochim. Acta*, 2015, **175**, 254–260.
36 L. C. Tomé, D. Mecerreyes, C. S. R. Freire, L. P. N. Rebelo and I. M. Marrucho, *J. Membr. Sci.*, 2013, **428**, 260–266.
37 J. G. Wijmans and R. W. Baker, *J. Membr. Sci.*, 1995, **107**, 1–21.
38 S. Matteucci, Y. Yampolskii, B. D. Freeman and I. Pinnau, *Materials Science of Membranes for Gas and Vapor Separation*, John Wiley & Sons, Ltd, 2006, pp. 1–47.
39 S. W. Rutherford and D. D. Do, *Adsorption*, 1997, **3**, 283–312.
40 E. Santos, J. Albo, C. I. Daniel, C. A. M. Portugal, J. G. Crespo and A. Irabien, *J. Membr. Sci.*, 2013, **430**, 56–61.
41 D. Morgan, L. Ferguson and P. Scovazzo, *Ind. Eng. Chem. Res.*, 2005, **44**, 4815–4823.
42 D. Camper, J. Bara, C. Koval and R. Noble, *Ind. Eng. Chem. Res.*, 2006, **45**, 6279–6283.
43 P. J. Carvalho and J. A. P. Coutinho, *J. Phys. Chem. Lett.*, 2010, **1**, 774–780.
44 M. S. Shannon, J. M. Tedstone, S. P. O. Danielsen, M. S. Hindman, A. C. Irvin and J. E. Bara, *Ind. Eng. Chem. Res.*, 2012, **51**, 5565–5576.
45 J. L. Anderson, J. K. Dixon and J. F. Brennecke, *Acc. Chem. Res.*, 2007, **40**, 1208–1216.
46 M. J. Muldoon, S. N. V. K. Aki, J. L. Anderson, J. K. Dixon and J. F. Brennecke, *J. Phys. Chem. B*, 2007, **111**, 9001–9009.
47 Y.-F. Hu, Z.-C. Liu, C.-M. Xu and X.-M. Zhang, *Chem. Soc. Rev.*, 2011, **40**, 3802–3823.
48 A. Tagiuri, K. Z. Sumon, A. Henni, K. Zanganeh and A. Shafeen, *Fluid Phase Equilib.*, 2014, **375**, 324–331.
49 M. Althuluth, M. T. Mota-Martinez, M. C. Kroon and C. J. Peters, *J. Chem. Eng. Data*, 2012, **57**, 3422–3425.
50 P. J. Carvalho, K. A. Kurnia and J. A. P. Coutinho, *Phys. Chem. Chem. Phys.*, 2016, **18**, 14757–14771.
51 L. M. Robeson, *J. Membr. Sci.*, 2008, **320**, 390–400.
52 C. M. S. S. Neves, K. A. Kurnia, K. Shimizu, I. M. Marrucho, L. P. N. Rebelo, J. A. P. Coutinho, M. G. Freire and J. N. Canongia Lopes, *Phys. Chem. Chem. Phys.*, 2014, **16**, 21340–21348.
53 P. Cserjési, N. Nemestóthy and K. Bélafi-Bakó, *J. Membr. Sci.*, 2010, **349**, 6–11.